Hindawi Publishing Corporation
International Journal of Superconductivity
Volume 2015, Article ID 273570, 9 pages
http://dx.doi.org/10.1155/2015/273570

Research Article

Spin Flows in Magnetic Semiconductor/Insulator/Superconductor Tunneling Junction

Michihide Kitamura and Akinobu Irie

Department of Electrical and Electronic System Engineering, Utsunomiya University, 7-1-2 Yoto, Utsunomiya, Tochigi 321-8585, Japan

Correspondence should be addressed to Michihide Kitamura; kitamura@cc.utsunomiya-u.ac.jp

Received 18 December 2014; Accepted 25 March 2015

Academic Editor: Zongqing Ma

Tunneling currents along the c-axis of the majority and minority spin electrons have been studied for a magnetic semiconductor (MS)/insulator (I)/superconductor (S) tunneling junction consisting of a $Ga_{1-x}Mn_xAs$ MS with $x = 1/32$, a nonmagnetic I with a realistic dimension, and a $HgBa_2Ca_2Cu_3O_{8.4}$ (Hg-1223) high-T_c S. The normalized charge and spin currents, $Q_{T,C}^{(\mu')}(V_{ex})$ and $Q_{T,S}^{(\mu')}(V_{ex})$, and the flows of the majority (↑) and minority (↓) spin electrons, $Q_{T,\uparrow}^{(\mu')}(V_{ex})$ and $Q_{T,\downarrow}^{(\mu')}(V_{ex})$, have been calculated at a fixed external voltage V_{ex}, as a function of the magnetic moment μ' ($\equiv \mu/\mu_B$) per a Mn atom which is deduced from the band structure calculations. It is found that the tunneling due to the minority spin electron dominates when $\mu' < 2.4$, but such a phenomenon is not found for $\mu' > 2.4$. We have pointed out that the present MS/I/S tunneling junction seems to work as a switching device in which the ↑ and ↓ spin flows can be easily controlled by the external magnetic field.

1. Introduction

Spintronics, in which both the charge and spin of an electron should be controlled, is one of the most attractive subjects in solid state physics and technology. Therefore, if one can make a device in which the spin flow can be easily controlled, then such a device may play an essential role in the field of the spintronics. By using ferromagnetic materials such as $3d$-transition metal compounds, spin-polarized electrons can be easily injected into the other materials including superconductors. In the nonsuperconducting states, a phenomenon such as the tunneling magnetoresistance (TMR) has been clearly observed in the magnetic tunneling junction (MTJ) consisting of two ferromagnetic (F) electrodes separated by an insulating (I) barrier, that is, F/I/F-junction. Parkin et al. [1] and Yuasa et al. [2] have measured very large TMR values for Fe/MgO/Fe junctions, and Belashchenko et al. [3] have theoretically studied the electronic structure and spin-dependent tunneling in epitaxial Fe/MgO/Fe(001) tunnel junctions and found that interface resonant states in Fe/MgO/Fe(001) tunnel junctions contribute to the conductance in the antiparallel configuration and are responsible for the decrease of TMR at a small barrier thickness, which explains the experimental results of Yuasa et al. [2].

Many studies have been done for the superconductor (S)/insulator (I)/superconductor (S) tunneling junctions, that is, Josephson junction, from the experimental and theoretical points of view. Barone and Paterno [4] presented to us a guide principle to study the Josephson effect. We have also studied the current- (I-) voltage (V) characteristics observed in the BSCCO intrinsic Josephson junctions from both the experimentally [5–8] and theoretically [9–11]. If a junction is made from F and S layers, the further interesting phenomena could be observed. For such junctions, there are two valuable review articles, one is by Golubov et al. [12] and the other is by Buzdin [13]. The one of the interesting phenomena found in a junction consisting of the ferromagnetic F and superconducting S layers could be an occurrence of the

S/F/S π-junction [14–21]. It has already been known that the π-junction is caused to the damped oscillatory behavior of the Cooper pair (CP) wave function in the ferromagnetic layer.

Very recently, we have theoretically studied the c-axis charge and spin currents in F/I/S tunneling junction [22], in which Hg-1223 copper-oxides high-T_c superconductor $HgBa_2Ca_2Cu_3O_{8.4}$ and a ferromagnetic Fe metal have been selected as the S and F layers. Our recent study [22] has showed that an interesting result such that the minority spin current exceeds the majority one is surely found in the junction consisting of the nonmagnetic insulating layer; however, more clear and remarkable result is found in the junction including the magnetic insulating layer. Magnetic insulator (MI) can be made by doping the magnetic impurities into the nonmagnetic insulator, but it may not be so easy to make a tunneling device such as F/MI/S junction whose magnetizations are in antiparallel configuration. In the present paper, therefore, we further study the magnetic semiconductor (MS)/insulator (I)/superconductor (S) tunneling junction. As S, the Hg-1223 copper-oxides high-T_c superconductor is selected again, and a $Ga_{1-x}Mn_xAs$ with $x = 1/32$ is selected as MS. For the ferromagnetic III-V semiconductors, there is an excellent article written by Ohno [23], in which he presented the properties of III-V-based ferromagnetic semiconductors (In,Mn)As and (Ga,Mn)As. Some of the interesting results obtained for the $Ga_{1-x}Mn_xAs$ MS are that (1) no ferromagnetism is observed below $x = 0.005$ and (2) the relation between x and the ferromagnetic transition temperature $T_c^{(F)}$ is found as $T_c^{(F)} \simeq 2000x \pm 10\,K$ up to $x = 0.05$. The x in the present study is fixed to $1/32 = 0.03125$, so that the $T_c^{(F)}$ of the present $Ga_{0.96875}Mn_{0.03125}As$ MS is calculated as $62.5 \pm 10\,K$. It is well known that the $Ga_{1-x}Mn_xAs$ MS shows some phases such as magnetic semiconductor, half-metal, and ferromagnetic metal due to the change of the magnetization, that is, the change of the external magnetic field. Therefore, it is expected that an interesting phenomenon could be observed in the current- (I-) voltage (V) characteristics of the present MS/I/S tunneling junction. This is a motivation of the use of MS.

The transition temperature T_c of Hg-based copper-oxides superconductors is fairly higher than the liquid nitrogen temperature T_{LN} (=77 K), so that the Hg-1223 high-T_c superconductor with $\delta = 0.4$, that is, $HgBa_2Ca_2Cu_3O_{8.4}$ whose T_c is 135 K, has been selected as a superconducting layer S. As already stated, the ferromagnetic transition temperature $T_c^{(F)}$ of $Ga_{1-x}Mn_xAs$ MS with $x = 1/32$ is calculated as about $60 \pm 10\,K$. Therefore, it is certain that the superconductivity of Hg-1223 high-T_c superconductor is fairly well kept at the temperature region below 70 K, since the T_c of the Hg-1223 high-T_c superconductor is 135 K. This is the reason why we have selected the Hg-1223 high-T_c superconductor as S layer.

The transport problem in the MS/S/MS tunneling junction has already been studied by Tao and Hu [24] and Shokri and Negarestani [25]. Here it should be noted that they have selected s-symmetry low-T_c superconductor as the S and adopted the Blonder-Tinkham-Klapwijk (BTK) model [26], which is based on the effective mass approximation. In the present paper, we consider the c-axis tunneling of the majority and minority spin electrons in $Ga_{0.96875}Mn_{0.03125}$ As MS/insulator I/$HgBa_2Ca_2Cu_3O_{8.4}$ high-T_c superconductor S tunneling junction within the framework of the tunneling Hamiltonian model. In the present junction, there are facts that (1) the electron states in the vicinity of the Fermi level E_F mainly come from $3d$ orbitals of Mn and Cu atoms, (2) the density of states (DOS) that originated from the $3d$ orbital shows a pointed structure meaning the localized nature, on the contrary to the DOS from s and p orbitals which show a broadened structure, that is, the extended nature, therefore, (3) the effective mass approximation, which is valid for the extended nature, may not be so good for the present system in which the electron states near the E_F are fairly well localized, and (4) the I layer is not a delta-functional but in a real dimensional size, whose barrier strength is large enough, so it must be noted that (5) the BTK model reaches the tunneling Hamiltonian model since the probability of Andreev reflection decreases with increasing the barrier strength of the I layer. The above are just a reason why we have adopted the tunneling Hamiltonian model based on the electrons with the Bloch states which are decided from the band structure calculations. It must be noted here that we do not set here a realistic size such as a width of the insulating layer. We think that it may be enough to state that the insulating layer works well as a tunneling barrier so that the tunneling Hamiltonian model is valid.

2. Theoretical

Tunneling current $i_{T,\sigma}(V)$ as a function of an applied voltage V of a ferromagnet- (F-) insulator- (I-) superconductor (S) tunneling junction is given by [22]

$$i_{T,\sigma}(V) = \frac{2\pi e}{\hbar}\widetilde{T}^2 \sum_{\mu_S}\sum_{L_S} \kappa_\sigma^{(F)}(\mu_S, L_S, V) \equiv i_{T,\sigma}^{(F)}(V), \quad (1)$$

$$\kappa_\sigma^{(F)}(\mu_S, L_S, V) = \eta_\sigma \sum_{\mathbf{k}_2}^{\Omega_S} \Theta_\sigma^{(F)}\left(\xi_{\mathbf{k}_2}^{(S)}, \Delta_{\mathbf{k}_2}, eV\right) \left|\lambda_{L_S}^{(\mu_S)}(\mathbf{k}_2)\right|^2, \quad (2)$$

where Ω_S is the first Brillouin zone of S. The $\lambda_{L_S}^{(\mu_S)}(\mathbf{k})$ is the coefficient in the expansion by the Bloch orbitals $\chi_{L_S}^{(\mu_S)}(\mathbf{k},\mathbf{r})$ of the total wave funtion $\Psi_\mathbf{k}(\mathbf{r})$ of S such that

$$\Psi_\mathbf{k}(\mathbf{r}) = \sum_{\mu_S}\sum_{L_S} \lambda_{L_S}^{(\mu_S)}(\mathbf{k})\, \chi_{L_S}^{(\mu_S)}(\mathbf{k},\mathbf{r}), \quad (3)$$

where μ_S and L_S are the site to be considered and the quantum state of atomic orbital of S, respectively.

As already stated in our previous paper [22], the η_σ is the tunneling probability of a σ-spin electron in the F/I/S tunneling junction defined by

$$\eta_\sigma = \frac{|T_\sigma|^2}{|T_\uparrow|^2 + |T_\downarrow|^2} \equiv \frac{|T_\sigma|^2}{\widetilde{T}^2}, \quad (4)$$

so that the value of η_σ strongly depends on the magnetic nature of an insulating layer I. It is clear that when the I shows no magnetic nature, the tunneling probabilities of majority and minority spin electrons should be equal; that is, $\eta_{\uparrow} = \eta_{\downarrow} = 1/2$, and when the I shows magnetic nature, those should differ from each other; that is, $\eta_{\uparrow} \neq \eta_{\downarrow}$. In the present study, only the nonmagnetic I layer is considered, so that the tunneling probabilities $\eta_{\uparrow}$ and $\eta_{\downarrow}$ of the majority and minority spin electrons are equal to each other; that is, only the case of $|T_{\uparrow}|^2 = |T_{\downarrow}|^2$ is considered here. As a tunneling process, coherent, incoherent, and WKB cases can be considered. In the present paper, the incoherent tunneling is mainly studied. The reason is described later.

In the incoherent tunneling case, the $\Theta_{\sigma}^{(F)}(\xi_{\mathbf{k}_2}^{(S)}, \Delta_{\mathbf{k}_2}, eV)$ in (2), which is written as $\Theta_{\sigma}^{(F)}(\xi_{\mathbf{k}_2}^{(S)}, \Delta_{\mathbf{k}_2}, eV)_{Inc}$, is given by [22]

$$\Theta_{\sigma}^{(F)}\left(\xi_{\mathbf{k}_2}^{(S)}, \Delta_{\mathbf{k}_2}, eV\right)_{Inc} = \left\{f\left(E_{\mathbf{k}_2} - eV\right) - f\left(E_{\mathbf{k}_2}\right)\right\} D_{\sigma}^{(F)}\left(E_{\mathbf{k}_2} - eV\right) + \left\{f\left(E_{\mathbf{k}_2}\right) - f\left(E_{\mathbf{k}_2} + eV\right)\right\} D_{\sigma}^{(F)}\left(-E_{\mathbf{k}_2} - eV\right), \quad (5)$$

where f is a Fermi-Dirac distribution function and $D_{\sigma}^{(F)}(x)$ is the TDOS of the ferromagnetic layer, that is, $Ga_{1-x}Mn_xAs$ with $x = 1/32$ MS layer, for σ spin state as a function of x. For the spin symbol σ used in our studies, it is noted that $\uparrow$ and $\downarrow$ mean the majority and minority spin electrons, respectively. The $E_{\mathbf{k}}$ is a quasiparticle excitation energy defined by $\sqrt{\xi_{\mathbf{k}}^2 + \Delta_{\mathbf{k}}^2}$, where the $\xi_{\mathbf{k}}$ is one electron energy relative to the Fermi level E_F and the $\Delta_{\mathbf{k}}$ is a superconducting energy gap given by $\Delta(T)\cos 2\theta_{\mathbf{k}}$.

The one electron energy $\xi_{\mathbf{k}}$ is calculated on the basis of the band theory using a universal tight-binding parameters (UTBP) method proposed by Harrison [27]. The energies of the atomic orbitals used in the band structure calculations have been calculated by using the spin-polarized self-consistent-field (SP-SCF) atomic structure calculations based on the Herman and Skillman prescription [28] using the Schwarz exchange correlation parameters [29]. The calculation procedure of the present band structure calculation is the same as that of our previous calculation [22]. Present band structure calculation for the $Ga_{1-x}Mn_xAs$ MS with $x = 1/32$ has been done using a unit cell consisting of 8 cubes such as a $2 \times 2 \times 2$-structure by a primitive cube. The unit cell includes 32 cations (=Ga or Mn) and 32 anions (=As); therefore, the condition $x = 1/32$ used in the present study means that the one of the 32 Ga atoms is replaced by Mn atom.

3. Results and Discussion

3.1. Density of States. The densities of states (DOSs) of $Ga_{1-x}Mn_xAs$ magnetic semiconductor MS with $x = 1/32$ have been calculated as a function of the d-electron configuration of Mn atom. The electron configuration used in the spin-polarized self-consistent-field (SP-SCF) atomic structure calculation for the Mn atom is $3d_{\uparrow}^{x}3d_{\downarrow}^{y}4s_{\uparrow}^{1}4s_{\downarrow}^{1}4p_{\uparrow}^{0}4p_{\downarrow}^{0}$ with $x + y = 5$, that for Ga atom is $4s_{\uparrow}^{1}4s_{\downarrow}^{1}4p_{\uparrow}^{0.5}4p_{\downarrow}^{0.5}$, and that for As atom is $4s_{\uparrow}^{1}4s_{\downarrow}^{1}4p_{\uparrow}^{1.5}4p_{\downarrow}^{1.5}$. The DOSs calculated by setting (x, y) to $(2.5, 2.5)$, $(2.75, 2.25)$, $(3, 2)$, $(3.25, 1.75)$, $(3.5, 1.5)$, $(3.75, 1.25)$, $(4, 1)$, $(4.25, 0.75)$, $(4.5, 0.5)$, $(4.75, 0.25)$, and $(5, 0)$ are shown in Figures 1(a), 1(b), 1(c), 1(d), 1(e), 1(f), 1(g), 1(h), 1(i), 1(j), and 1(k), respectively. Resultant magnetic moment μ/μ_B calculated per Mn atom is 0.246, 0.480, 0.980, 1.972, 3.340, 3.514, 3.684, 3.849, 4.021, and 4.128 for (b), (c), (d), (e), (f), (g), (h), (i), (j), and (k), respectively. Calculated DOSs clearly show that (a) is a nonmagnetic semiconductor, (b) is a ferromagnetic semiconductor, (c) is a ferromagnetic zero-gap semiconductor, (d) and (e) are ferromagnetic metals, (f) and (g) are half-metals, and (h), (i), (j), and (k) are ferromagnetic metals. The phase change mentioned above is closely related to the energy position of the e_2-band of the minority spin electron denoted as $e_{2\downarrow}$-band. Actually, we can see that the $e_{2\downarrow}$-band of (d) locates below the Fermi level E_F, that of (e) is very close to the E_F, and that of (f) locates above the E_F. The energy shift of the $e_{2\downarrow}$-band makes the rapid change of the magnetization of the $Ga_{1-x}Mn_xAs$ MS. Such a rapid change in the magnetic moment is really observed between (d) and (f).

Finally, it is noted that the DOS of Hg-1223 high-T_c superconductor with $\delta = 0.4$, that is, $HgBa_2Ca_2Cu_3O_{8.4}$ with $T_c = 135$ K, has already been given in our recent paper [22].

3.2. Spin Flow. First of all, we did calculations for two cases in which the sample temperature T_{samp} has been set to 5 and 60 K. The BCS curve gives the values of 75 and 73.3 meV as the amplitudes $\Delta(T)$ of superconducting gap at $T_{samp} = 5$ and 60 K, respectively. The difference between these two values is small, so we have found that there is no significant difference between the current- (I-) voltage (V) characteristics calculated for these two temperatures, as is expected. In the following, therefore, the T_{samp} is set to 5 K. Here note that the magnetic field dependence of the magnetization of $Ga_{1-x}Mn_xAs$ MS with $x = 0.035$ has already been measured at 5 K by Ohno [23].

The calculations for the coherent and WKB cases need a very large CPU time as compared with the incoherent one [22]. Therefore, first, the I-V characteristics for *a* given 3d electron configuration, that is, *a* resultant magnetic moment, have been calculated for the coherent, incoherent, and WKB cases. As a result, we have found that the results calculated for three cases are fairly similar to each other. In the following, therefore, only the incoherent tunneling case is considered because of the CPU times in the numerical calculations.

The normalized charge and spin currents, $i_T^{(+)}(V)_{Nor}$ and $i_T^{(-)}(V)_{Nor}$, calculated for the present MS/I/S tunneling junction are shown in Figure 2. Here note that the $i_T^{(+)}(V)_{Nor}$ and $i_T^{(-)}(V)_{Nor}$ have already been defined by (11) in our recent paper [22] and that the MS used in (a) to (k) in Figure 2 is the same as that in (a) to (k) in Figure 1. Figure 2 clearly shows that the charge and spin currents are changed due to the change of the magnetization of MS. In order to directly see the currents due to the majority ($\uparrow$) and minority ($\downarrow$) spin electrons, we have drawn in Figure 3 the normalized currents calculated for the $\uparrow$ and $\downarrow$ spin electrons, $i_{T,\uparrow}(V)_{Nor}$ and $i_{T,\downarrow}(V)_{Nor}$. Here note that the normalized current $i_{T,\sigma}(V)_{Nor}$ is equal to $\sum_{\mu_S}\sum_{L_S}\kappa_{\sigma}^{(F)}(\mu_S, L_S, V)_{Nor}$ defined by (12) in our

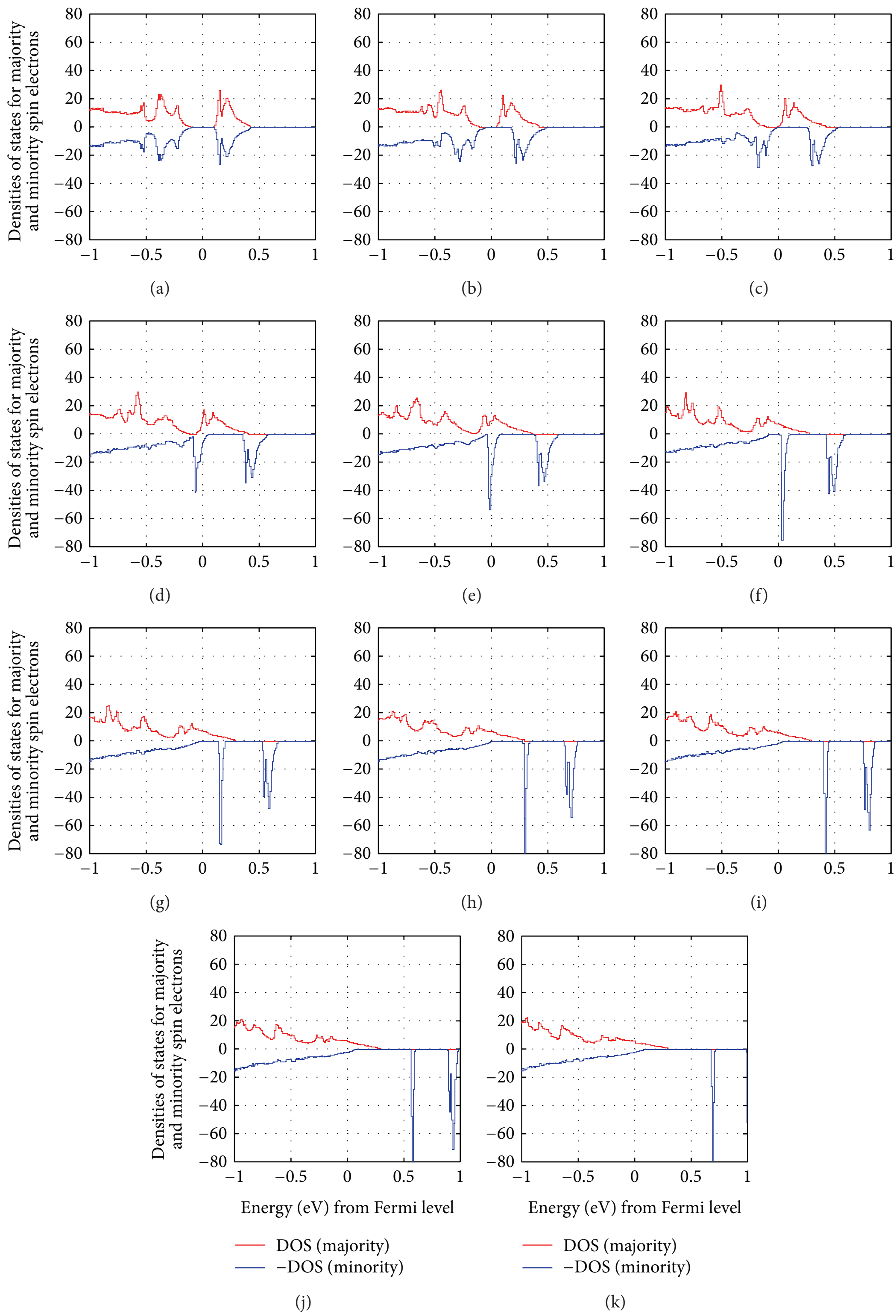

FIGURE 1: Densities of states (DOSs) calculated for $Ga_{1-x}Mn_xAs$ magnetic semiconductor MS with $x = 1/32$. The electron configuration used in the spin-polarized self-consistent-field (SP-SCF) atomic structure calculation for Mn atom is $3d_{\uparrow}^{x}3d_{\downarrow}^{y}4s_{\uparrow}^{1}4s_{\downarrow}^{1}4p_{\uparrow}^{0}4p_{\downarrow}^{0}$ with $x + y = 5$, that for Ga atom is $4s_{\uparrow}^{1}4s_{\downarrow}^{1}4p_{\uparrow}^{0.5}4p_{\downarrow}^{0.5}$, and that for As atom is $4s_{\uparrow}^{1}4s_{\downarrow}^{1}4p_{\uparrow}^{1.5}4p_{\downarrow}^{1.5}$. (a), (b), (c), (d), (e), (f), (g), (h), (i), (j), and (k) are the results calculated for $(x, y) = (2.5, 2.5)$, $(2.75, 2.25)$, $(3, 2)$, $(3.25, 1.75)$, $(3.5, 1.5)$, $(3.75, 1.25)$, $(4, 1)$, $(4.25, 0.75)$, $(4.5, 0.5)$, $(4.75, 0.25)$, and $(5, 0)$, respectively. Magnetic moment μ/μ_B calculated per Mn atom is 0.246, 0.480, 0.980, 1.972, 3.340, 3.514, 3.684, 3.849, 4.021, and 4.128 for (b), (c), (d), (e), (f), (g), (h), (i), (j), and (k), respectively. Present results show that (a) is a nonmagnetic semiconductor, (b) is a ferromagnetic semiconductor, (c) is a ferromagnetic zero-gap semiconductor, (d) and (e) are ferromagnetic metals, (f) and (g) are half-metals, and (h), (i), (j), and (k) are ferromagnetic metals.

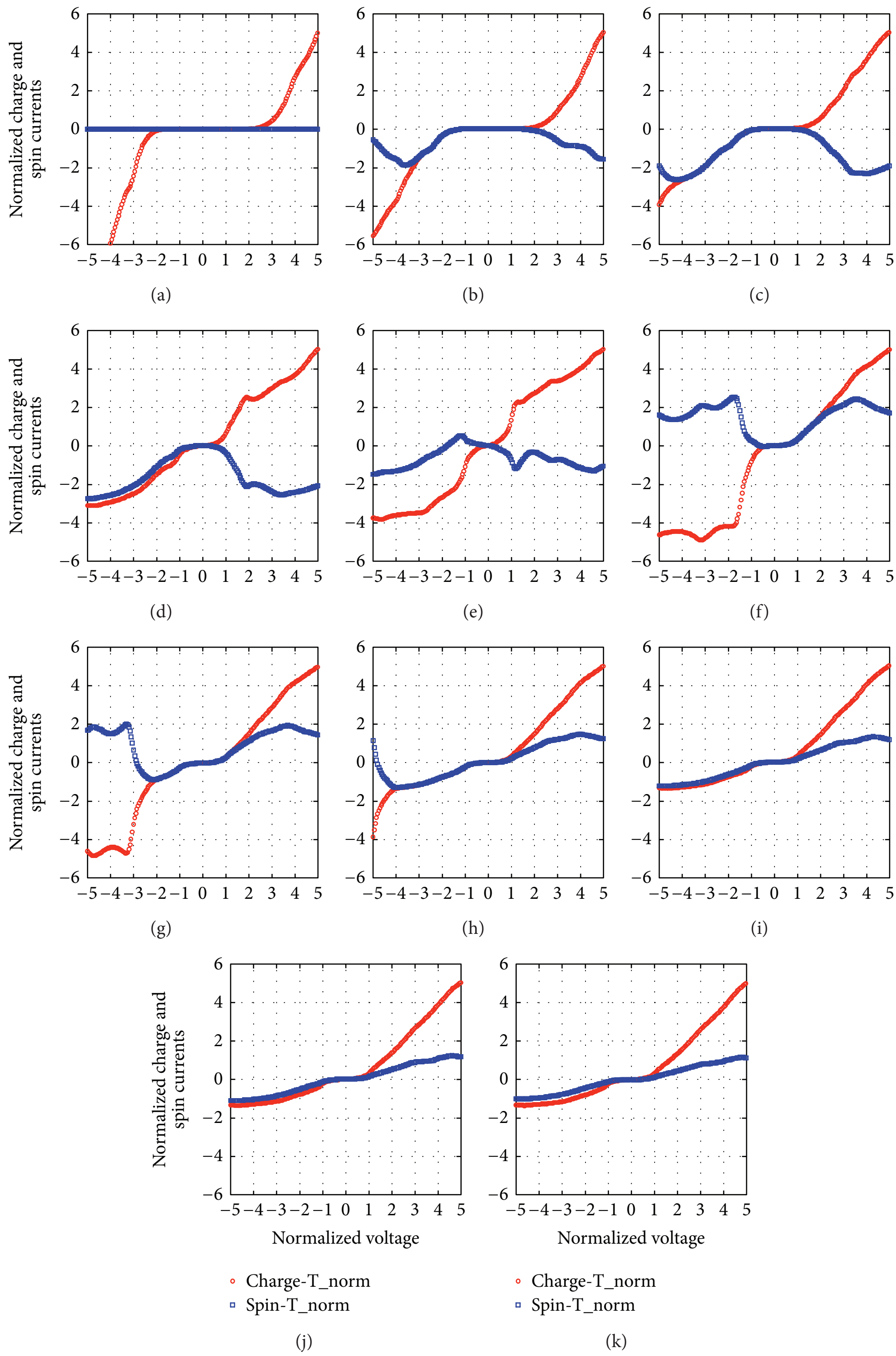

FIGURE 2: Normalized charge and spin currents $i_T^{(+)}(V)_{\text{Nor}}$ and $i_T^{(-)}(V)_{\text{Nor}}$ calculated for MS/I/S tunneling junction, where the MS is $Ga_{1-x}Mn_xAs$ with $x = 1/32$ and the S is Hg-1223 high-T_c superconductor with $\delta = 0.4$. The MS used in (a) to (k) is the same as that in (a) to (k) in Figure 1. The normalized voltage is defined by $eV/\Delta(T)$. Note that $\Delta(5) = 75$ meV.

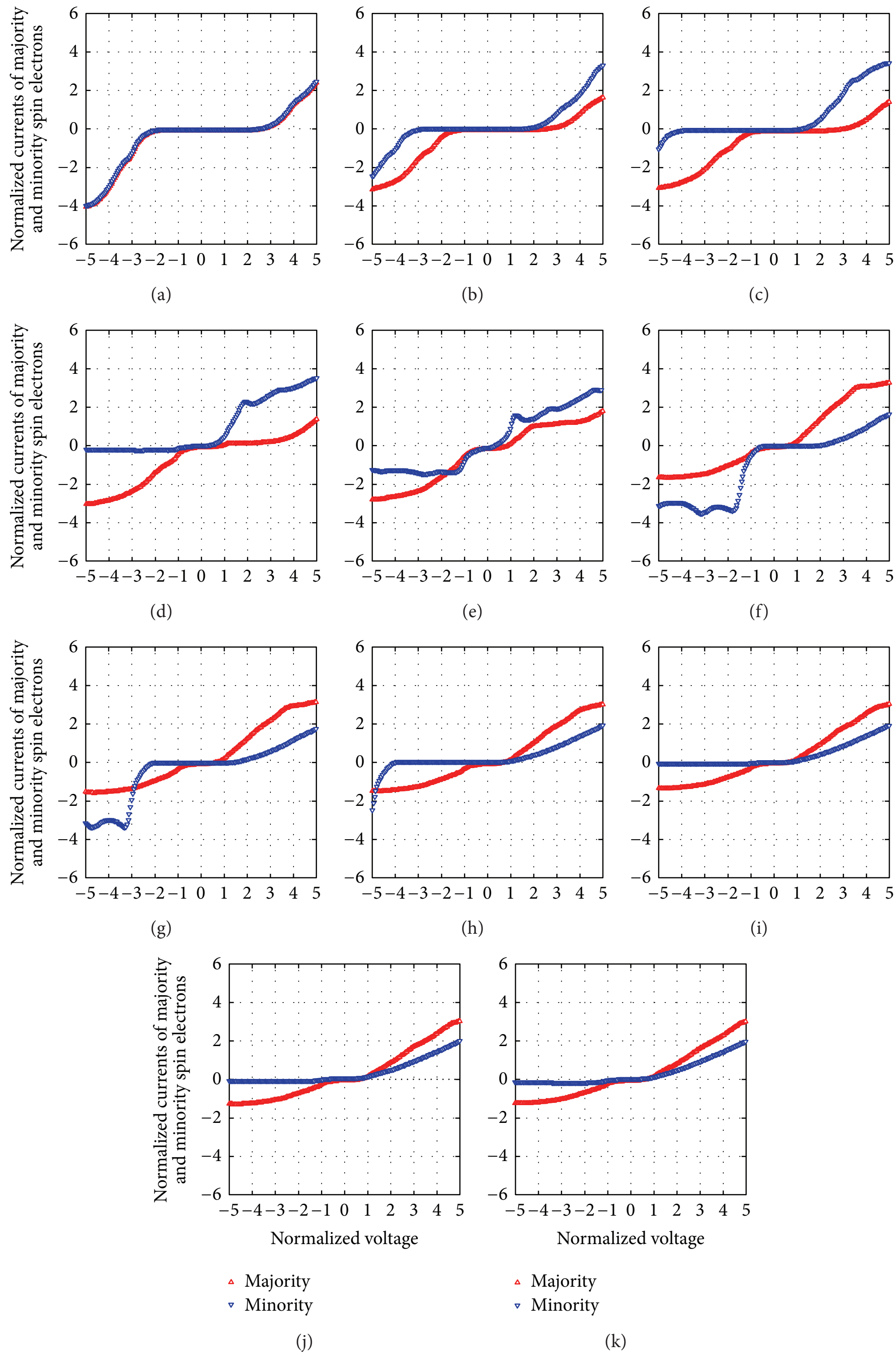

FIGURE 3: Normalized currents $i_{T,\uparrow}(V)_{\text{Nor}}$ and $i_{T,\downarrow}(V)_{\text{Nor}}$ calculated for the majority (↑) and minority (↓) spin electrons. (a) to (k) correspond to those in Figure 2. The normalized voltage is defined by $eV/\Delta(T)$, where $\Delta(5) = 75$ meV.

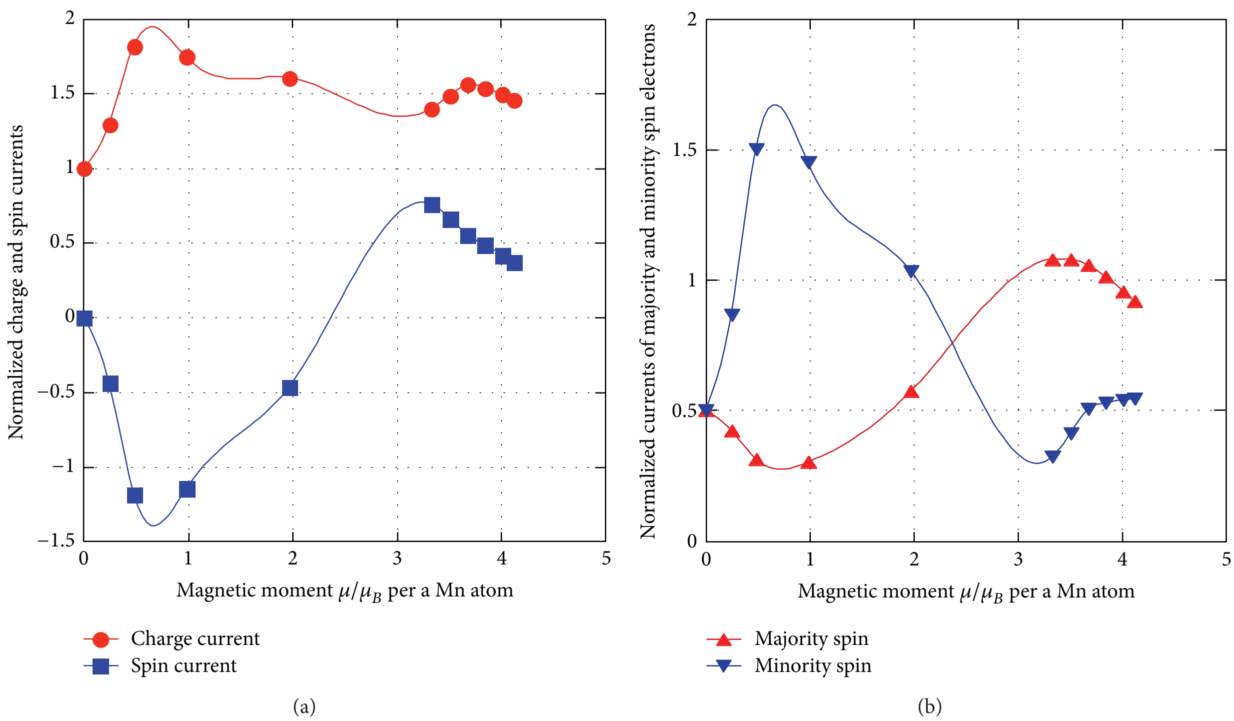

FIGURE 4: (a) Normalized charge and spin currents, $Q_{T,C}^{(\mu')}(V_{\text{ex}})$ and $Q_{T,S}^{(\mu')}(V_{\text{ex}})$, defined by (6) and (b) flows of the majority (↑) and minority (↓) spin electrons, $Q_{T,\uparrow}^{(\mu')}(V_{\text{ex}})$ and $Q_{T,\downarrow}^{(\mu')}(V_{\text{ex}})$. Those have been calculated as a function of μ', where μ' is the magnetic moment μ/μ_B calculated for Mn atom. The V_{ex} is the normalized voltage applied to the MS/I/S tunneling junction, which has been set to 4, that is, 300 (= 4 × 75) mV in real voltage. Note that relations $Q_{T,\uparrow}^{(\mu')}(V_{\text{ex}}) = (Q_{T,C}^{(\mu')}(V_{\text{ex}}) + Q_{T,S}^{(\mu')}(V_{\text{ex}}))/2$ and $Q_{T,\downarrow}^{(\mu')}(V_{\text{ex}}) = (Q_{T,C}^{(\mu')}(V_{\text{ex}}) - Q_{T,S}^{(\mu')}(V_{\text{ex}}))/2$ are held.

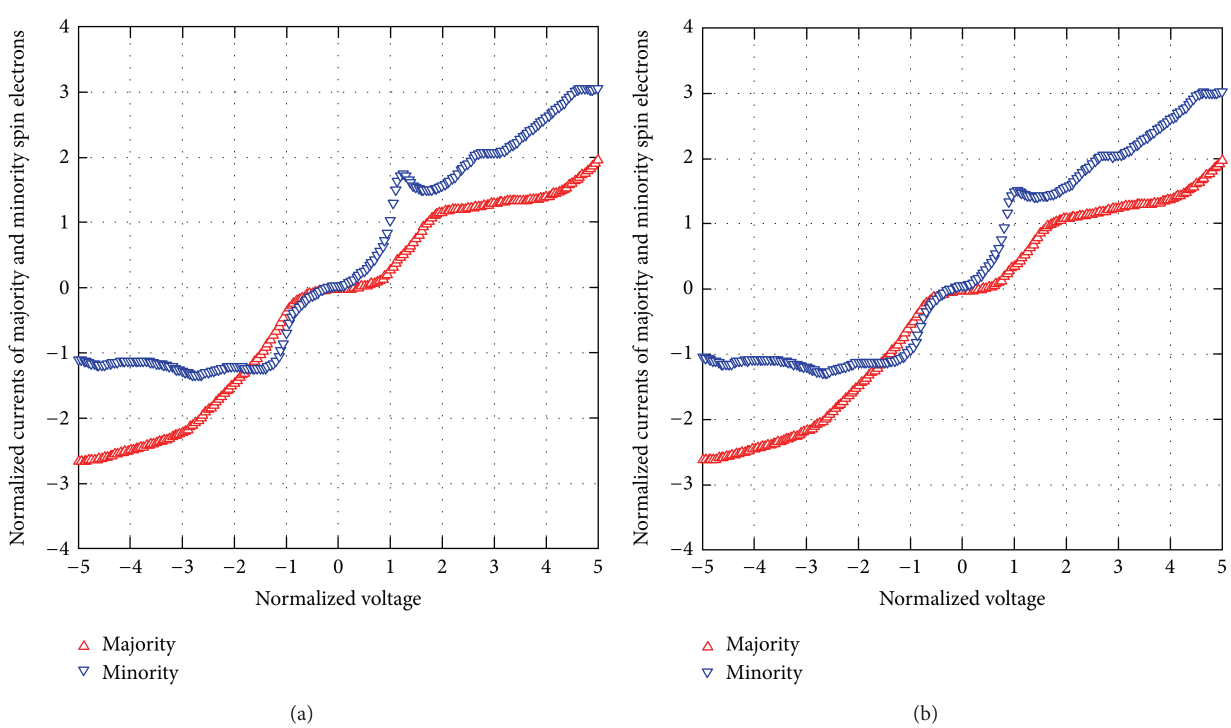

FIGURE 5: Normalized currents $i_{T,\uparrow}(V)_{\text{Nor}}$ and $i_{T,\downarrow}(V)_{\text{Nor}}$ calculated for the majority (↑) and minority (↓) spin electrons. (a) is the same as Figure 3(e); that is, the magnetic moment μ/μ_B per Mn atom is 1.972 and ζ is 1. (b) is the same as (a) but the ζ has been set to 0.8; that is, the normalized currents shown in (b) include the nonequilibrium effect.

previous paper [22], so that a relation $i_T^{(\pm)}(V)_{\text{Nor}} = i_{T,\uparrow}(V)_{\text{Nor}} \pm i_{T,\downarrow}(V)_{\text{Nor}}$ is satisfied. (a) to (k) in Figure 3 correspond to those in Figure 2. Figure 3 shows that the tunneling nature changes due to the change of the magnetic moment, that is, the magnetization of $Ga_{1-x}Mn_xAs$ MS. For example, if the normalized voltage is fixed to 4, then we can see in (b), (c), (d), and (e) an interesting result such that the tunneling current due to the ↓ spin electron is larger than the ↑ one, but such a result is not found in (f), (g), (h), (i), (j), and (k). It is clear that the result is closely related to the electronic structural change of MS which causes the change of the magnetization.

Experimentally, it may be possible to observe the external magnetic field dependence of the tunneling current at a fixed external voltage V_{ex}. In order to reproduce such an experimental situation, we have calculated the magnetic moment dependence of charge and spin currents. The normalized charge current $Q_{T,C}^{(\text{F})}(V_{\text{ex}})$ for the present purpose is defined by

$$Q_{T,C}^{(\text{F})}(V_{\text{ex}}) \equiv \frac{\sum_\sigma i_{T,\sigma}^{(\text{F})}(V_{\text{ex}})}{\sum_\sigma i_{T,\sigma}^{(\text{NM})}(V_{\text{ex}})} = \frac{\sum_\sigma \sum_{\mu_S} \sum_{L_S} \kappa_\sigma^{(\text{F})}(\mu_S, L_S, V_{\text{ex}})}{\sum_\sigma \sum_{\mu_S} \sum_{L_S} \kappa_\sigma^{(\text{NM})}(\mu_S, L_S, V_{\text{ex}})} \equiv Q_{T,C}^{(\mu')}(V_{\text{ex}}). \quad (6)$$

Here NM means the nonmagnetic phase, so that the magnetic moment μ/μ_B ($\equiv \mu'$) per Mn atom is 0. F means the ferromagnetic phase; therefore, in the following, the symbol F is replaced by the symbol μ'. Using (6), we can calculate the normalized charge current $Q_{T,C}^{(\mu')}(V_{\text{ex}})$ as a function of μ'. The raw values of $\sum_{\mu_S} \sum_{L_S} \kappa_\uparrow^{(\text{F})}(\mu_S, L_S, V_{\text{ex}})$ and $\sum_{\mu_S} \sum_{L_S} \kappa_\downarrow^{(\text{F})}(\mu_S, L_S, V_{\text{ex}})$ have already been calculated numerically, so that the ratio of those raw values is easily given. As a result, we can get the normalized spin current $Q_{T,S}^{(\mu')}(V_{\text{ex}})$ as a function of μ'. The calculated normalized charge and spin currents, $Q_{T,C}^{(\mu')}(V_{\text{ex}})$ and $Q_{T,S}^{(\mu')}(V_{\text{ex}})$, are shown in Figure 4(a) as a function of the calculated μ'. By using the above $Q_{T,C}^{(\mu')}(V_{\text{ex}})$ and $Q_{T,S}^{(\mu')}(V_{\text{ex}})$, we can easily get the flows $Q_{T,\uparrow}^{(\mu')}(V_{\text{ex}})$ and $Q_{T,\downarrow}^{(\mu')}(V_{\text{ex}})$ of the majority (↑) and minority (↓) spin electrons. Those are shown in Figure 4(b) as a function of μ'. Figure 4 shows that the nature of the spin flow is changed at the μ' with the value around 2.4. Namely, the tunneling due to the minority spin electron dominantly occurs when $\mu' < 2.4$, but for the case of $\mu' > 2.4$, such a tunneling phenomenon is not found. It is certain that such a change is closely related to the variation of the $e_{2\downarrow}$-band of the $Ga_{1-x}Mn_xAs$ MS. The value of the magnetization M can be easily controlled by the external magnetic field B_{ext}. The M-B_{ext} curve at 5 K of $Ga_{1-x}Mn_xAs$ MS with $x = 0.035$ has already been drawn in Figure 3 in Ohno's paper [23], which clearly shows that the $B_{\text{ext}} = 0.02$ T is a large external magnetic field enough to get the saturation of the magnetization. Here note that we have checked that the magnetic induction with the value of 0.02 T has no considerable effect on the present superconductor.

3.3. Effect of Nonequilibrium. We are now considering the superconductors consisting of Cooper pairs (CPs) with a spin-singlet state. In the junctions involving the ferromagnetic materials and the superconductors, therefore, it is easily supposed that the unbalance in the numbers of the ↑ and ↓ spin electrons makes a decrease in the number of the CPs. This is just a nonequilibrium effect. The decrease in the number of CPs makes a decrease in the amplitude $\Delta(T)$ of the superconducting gap. Therefore, in order to take into account the influence of such a nonequilibrium effect, we have introduced a parameter ζ with a range of $0 < \zeta \leq 1$, by which the $\Delta(T)$ is reduced to $\zeta\Delta(T)$. It is clear that the case of $\zeta = 1$ means no consideration for the nonequilibrium effect.

Figure 1(e) shows that the Fermi level just locates on the $e_{2\downarrow}$-band with a pointed shape, so that a sizable unbalance in the numbers of the ↑ and ↓ spin electrons could be found in this case. Nevertheless, the nonequilibrium effect should not be so large; therefore, as an attempt we have calculated the I-V characteristics by setting ζ to 0.8. The normalized currents calculated for $\zeta = 1$ and 0.8 are shown in Figures 5(a) and 5(b), respectively. Apart from the reliability of the value of 0.8, the calculated results have showed that there is no significant difference between them. The above result tells us that a considerable nonequilibrium effect could not be found in the I-V characteristics of the MS/I/S tunneling junction studied here. This means that the present MS/I/S tunneling junction stably works as a device to switch the ↑ and ↓ spin flows by varying the B_{ext} within the range of $|B_{\text{ext}}| < 0.02$ T.

4. Summary

The c-axis tunneling of the majority and minority spin electrons has been studied for the MS/I/S tunneling junction consisting of $Ga_{1-x}Mn_xAs$ magnetic semiconductor MS with $x = 1/32$, an insulator I with a realistic dimension, and $HgBa_2Ca_2Cu_3O_{8.4}$ (Hg-1223) high-T_c superconductor S. We have deduced the magnetic moment μ' ($\equiv \mu/\mu_B$) per Mn atom from the band structure calculations for the $Ga_{1-x}Mn_xAs$ MS and calculated the normalized charge and spin tunneling currents, $Q_{T,C}^{(\mu')}(V_{\text{ex}})$ and $Q_{T,S}^{(\mu')}(V_{\text{ex}})$, and the flows of the majority (↑) and minority (↓) spin electrons, $Q_{T,\uparrow}^{(\mu')}(V_{\text{ex}})$ and $Q_{T,\downarrow}^{(\mu')}(V_{\text{ex}})$, as a function of μ' at a given external voltage V_{ex}. We have found that the tunneling due to the minority spin electron dominantly occurs when $\mu' < 2.4$, but such a phenomenon is not found in the case of $\mu' > 2.4$. We have pointed out that the present MS/I/S tunneling junction seems to work as a switching device in which the ↑ and ↓ spin flows can be easily controlled by varying slightly the external magnetic field.

Conflict of Interests

The authors declare that there is no conflict of interests regarding the publication of this paper.

References

[1] S. S. P. Parkin, C. Kaiser, A. Panchula et al., "Giant tunnelling magnetoresistance at room temperature with MgO (100) tunnel barriers," *Nature Materials*, vol. 3, no. 12, pp. 862–867, 2004.

[2] S. Yuasa, T. Nagahama, A. Fukushima, Y. Suzuki, and K. Ando, "Giant room-temperature magnetoresistance in single-crystal Fe/MgO/Fe magnetic tunnel junctions," *Nature Materials*, vol. 3, no. 12, pp. 868–871, 2004.

[3] K. D. Belashchenko, J. Velev, and E. Y. Tsymbal, "Effect of interface states on spin-dependent tunneling in Fe/MgO/Fe tunnel junctions," *Physical Review B*, vol. 72, Article ID 140404, 2005.

[4] A. Barone and G. Paterno, *Physics and Applications of the Josephson Effects*, John Wiley & Sons, New York, NY, USA, 1982.

[5] A. Irie, S. Heim, S. Schromm et al., "Critical currents of small $Bi_2Sr_2CaCu_2O_{8+x}$ intrinsic Josephson junction stacks in external magnetic fields," *Physical Review B*, vol. 62, p. 6681, 2000.

[6] A. Irie, G. Oya, R. Kleiner, and P. Müller, "Transport properties of small-sized intrinsic Josephson junctions in $Bi_2Sr_2CaCu_2O_y$," *Physica C: Superconductivity*, vol. 362, no. 1–4, pp. 145–149, 2001.

[7] A. Irie, N. Arakawa, H. Sakuma, M. Kitamura, and G. Oya, "Magnetization-dependent critical current of intrinsic Josephson junctions in Co/Au/Bi," *Journal of Physics: Conference Series*, vol. 234, no. 4, Article ID 042015, 2010.

[8] A. Irie, M. Otsuka, K. Murata, K. Yamaki, and M. Kitamura, "Influence of spin injection on the in-plane and out-of-plane transport properties of BSCCO single crystal," *IEEE Transactions on Applied Superconductivity*, vol. 25, no. 3, Article ID 1800404, 2014.

[9] M. Kitamura, A. Irie, and G.-I. Oya, "Quasiparticle tunneling current-voltage characteristics of intrinsic Josephson junctions in $Bi_2Sr_2CaCu_2O_{8+\delta}$," *Physical Review B*, vol. 66, Article ID 054519, 2002.

[10] M. Kitamura, A. Irie, and G. Oya, "Conditions for observing Shapiro steps in a $Bi_2Sr_2CaCu_2O_{8+\delta}$ high-T_c superconductor intrinsic Josephson junction: numerical calculations," *Physical Review B*, vol. 76, Article ID 064518, 2007.

[11] M. Kitamura, A. Irie, and G. Oya, "Shapiro steps in $Bi_2Sr_2CaCu_2O_{8+\delta}$ intrinsic Josephson junctions in magnetic field," *Journal of Applied Physics*, vol. 104, no. 6, Article ID 063905, 2008.

[12] A. A. Golubov, M. Y. Kupriyanov, and E. Il'ichev, "The current-phase relation in Josephson junctions," *Reviews of Modern Physics*, vol. 76, no. 2, pp. 411–469, 2004.

[13] A. I. Buzdin, "Proximity effects in superconductor-ferromagnet heterostructures," *Reviews of Modern Physics*, vol. 77, no. 3, pp. 935–976, 2005.

[14] A. V. Andreev, A. I. Buzdin, and R. M. Osgood III, "Phase in magnetic-layered superconductors," *Physical Review B*, vol. 43, no. 13, pp. 10124–10131, 1991.

[15] V. Prokić, A. I. Buzdin, and L. Dobrosavljević-Grujić, "Theory of the π junctions formed in atomic-scale superconductor/ferromagnet superlattices," *Physical Review B*, vol. 59, article 587, 1999.

[16] V. V. Ryazanov, V. A. Oboznov, A. Y. Rusanov, A. V. Veretennikov, A. A. Golubov, and J. Aarts, "Coupling of two superconductors through a ferromagnet: evidence for a π junction," *Physical Review Letters*, vol. 86, article 2427, 2001.

[17] T. Kontos, M. Aprili, J. Lesueur, F. Genêt, B. Stephanidis, and R. Boursier, "Josephson junction through a thin ferromagnetic layer: negative coupling," *Physical Review Letters*, vol. 89, Article ID 137007, 2002.

[18] W. Guichard, M. Aprili, O. Bourgeois, T. Kontos, J. Lesueur, and P. Gandit, "Phase sensitive experiments in ferromagnetic-based Josephson junctions," *Physical Review Letters*, vol. 90, no. 16, Article ID 167001, 4 pages, 2003.

[19] V. A. Oboznov, V. V. Bol'ginov, A. K. Feofanov, V. V. Ryazanov, and A. I. Buzdin, "Thickness dependence of the Josephson ground states of superconductor-ferromagnet-superconductor junctions," *Physical Review Letters*, vol. 96, no. 19, Article ID 197003, 2006.

[20] J. W. A. Robinson, S. Piano, G. Burnell, C. Bell, and M. G. Blamire, "Critical current oscillations in strong ferromagnetic π junctions," *Physical Review Letters*, vol. 97, no. 17, Article ID 177003, 2006.

[21] M. Weides, M. Kemmler, H. Kohlstedt et al., "0-π Josephson tunnel junctions with ferromagnetic barrier," *Physical Review Letters*, vol. 97, no. 24, Article ID 247001, 2006.

[22] M. Kitamura, Y. Uchiumi, and A. Irie, "Charge and spin currents in ferromagnet-insulator-superconductor tunneling junctions using Hg-1223 high-T_c superconductor," *International Journal of Superconductivity*, vol. 2014, Article ID 957045, 15 pages, 2014.

[23] H. Ohno, "Properties of ferromagnetic III–V semiconductors," *Journal of Magnetism and Magnetic Materials*, vol. 200, no. 1–3, pp. 110–129, 1999.

[24] Y. C. Tao and J. G. Hu, "Coherent transport and Andreev reflection in ferromagnetic semiconductor/superconductor/ferromagnetic semiconductor double tunneling junctions," *Physical Review B*, vol. 72, Article ID 165329, 2005.

[25] A. Shokri and S. Negarestani, "Spin dependent transport in diluted magnetic semiconductor/superconductor tunnel junctions," *Physica C: Superconductivity and Its Applications*, vol. 507, pp. 75–80, 2014.

[26] G. E. Blonder, M. Tinkham, and T. M. Klapwijk, "Transition from metallic to tunneling regimes in superconducting microconstrictions: excess current, charge imbalance, and supercurrent conversion," *Physical Review B*, vol. 25, article 4515, 1982.

[27] W. A. Harrison, *Elementary Electronic Structure*, World Scientific Publishers, Singapore, 1999.

[28] F. Herman and S. Skillman, *Atomic Structure Calculations*, Prentice-Hall, Englewood Cliffs, NJ, USA, 1999.

[29] K. Schwarz, "Optimization of the statistical exchange parameter α for the free atoms H through Nb," *Physical Review B*, vol. 5, no. 7, pp. 2466–2468, 1972.